ASM Sc. J., 14, 2021
https://doi.org/10.32802/asmscj.2020.488

Stability and Transportation of Iron Oxide Nanoparticles in Subsurface Water and Soil

Nur Suraya Ahmad*, Shahidan Radiman[1] and Wan Zuhairi Wan Yaacob[2]

[1]*Pusat Pengajian Fizik Gunaan, Fakulti Sains & Teknologi, Universiti Kebangsaan Malaysia, Bangi, Selangor, Malaysia*

[2]*Pusat Pengajian Sains Sekitaran dan Sumber Alam, Fakulti Sains & Teknologi, Universiti Kebangsaan Malaysia, Bangi, Selangor, Malaysia*

Iron oxide nanoparticles are utilised in a broad range of applications (magnetic data storage, biosensing, drug delivery, treatment and remediation of contaminated soil and groundwater); causing noticeable quantities of iron oxide nanoparticles to be released into the environment. In this study, aggregation and stability of iron oxide nanoparticles in water were investigated within the range of pH 3 – pH 9 at a constant concentration of iron oxide nanoparticles and humic acid. The pH of the solution was selected to be continuously monitored at pH 7 to investigate the transportation and deposition behaviour of iron oxide nanoparticles in porous media at different velocities. It was found that iron oxide nanoparticles were aggregated and settle down as settled particles at low pH (pH 3 – pH 5). Iron oxide nanoparticles were stable, mobile and transported at a high pH, which is the pH range of natural water (pH 6.5 – pH 8.5). Iron oxide nanoparticles were strongly attached to the silica sand at natural water velocity in porous media, which is 2.93 ml min^{-1}. Overall, the presence of humic acid in aquifers and porous media, the pH range of natural water (pH 6.5 – pH 8.5) and the slow speed (2.93 ml min^{-1}) of water are expected to be a key factor that enhances the stability and mobility of iron oxide nanoparticles in natural water and porous media.

Keywords: iron oxide nanoparticles; DLVO; attachment efficiency; stability

I. INTRODUCTION

The nanotechnology market is developing rapidly, and new applications for nanoparticles are constantly emerging. Rapid nanotechnology development poses significant and uncertain risks to the environment and public health, especially as more nanoparticles make their way to the marketplace. Several past research showed nanoparticles could enter the environment during the production of raw material and nano-enabled products, product use and after disposal of nanoparticles-containing products (waste handling) (Chowdhury *et al.*, 2011; Petosa *et al.*, 2012; Bundschuh *et al.*, 2018). In addition, nanoparticles also may exhibit greater mobility upon releases and have the potential to be transported in the subsurface. For instance, nanoparticles can move into the surface water, subsurface and groundwater through soil layer (Jeong & Kim 2009) and enter into the food web through bioaccumulation (Chowdhury *et al.*, 2011). This entire scenario created a huge dilemma when it comes to public health prevention as nanoparticles can enter the human food chain or drinking water.

Nanoparticles can naturally be founded in the environment, but they often disappeared from the environment by natural process. However, this situation was different with manufactured/engineered nanoparticles that will be surface-functionalised, stabilised or matrix embedded. Manufactured nanoparticles in the environment may undergo interaction such as physical, chemical and biological transformation (Omar *et al.*, 2014). These interactions are expected to control the fate and behaviours of nanoparticles in the environment. Some manufactured nanoparticles may contain toxic components and can significantly affect the environment.

*Corresponding author's e-mail: nursuraya_ahmad@siswa.ukm.edu.my

Therefore, it is important to understand nanoparticles interaction with natural water components such as natural colloids and natural water. In short, natural colloids are ubiquitous (Yang & Xing 2009), and one of the major components of natural colloids is natural organic matter. Nanoparticles stability in the aquatic and subsurface environment is also influenced by the presence of natural organic matter (Godinez & Darnault 2011). Natural organic matter is a large organic compounds family (Klaine *et al.*, 2008; Wagner *et al.*, 2014) and approximately 50-80% of the natural organic matter in natural water are made up by humic substances (Buffle *et al.*, 1998). Humic acid can act as a natural dispersant (Peijnenburg *et al.*, 2015), has a stabilising effect on most nanoparticles and present anywhere in aquatic systems. Adsorption of humic acid on nanoparticles will enhance toxicity to aquatic life due to the dispersion of small particles in natural water (Hoecke *et al.*, 2011)

Nanoparticles that are exposed to the environment may undergo surface modifications, depending on the concentration of humic acid (Ghosh *et al.*, 2010) and has a high impact on the transportation of low solubility contaminant due to aggregation and stabilisation (Chekli *et al.*, 2013a). Once adsorption of humic acid nanoparticles was formed, they will be able to undergo an aggregation due to the interaction with other natural nanoparticles or larger particles (Ju-Nam & Lead 2008). Humic acid has a stabilising effect on most nanoparticles (Frimmel *et al.*, 2010) and adsorption of humic acid on nanoparticles will enhance the toxicity of aquatic life due to the dispersion of small particles in natural water (Hoecke *et al.*, 2011).

Moreover, the stability controls the transportation and fates of nanoparticles in natural porous media (soils and groundwater aquifer) and natural water systems (lake, rivers). Nanoparticles stability is achieved when the small particles stay separate from each other (Dickson *et al.*, 2012) and have the ability to remain in suspensions (Hu *et al.*, 2010). For instance, nanoparticles which are less than 100 nm, Brownian diffusion will take control of the long-range forces between individual nanoparticles, causing collisions between particles. When the contact occurs, it can result in attachment or repulsion (Hotze *et al.*, 2010)

Previous research on fate and behaviour of iron oxide nanoparticles can be have been reported in this literature (Baalousha *et al.*, 2008, Baalousha 2009, Chekli *et al.*, 2013a; 2013b, Nur *et al.*, 2019). They state that the factors that influenced the aggregation and stability of iron oxide are pH, nanoparticles concentration and natural organic concentration. Therefore, the objective of this study are (1) to investigate the aggregation and stability (physical transformation) of iron oxide nanoparticles in the presence of humic acid by considering a wide range pH variation in solution, (2) to investigate the attachment and deposition of nanoparticles in porous media (silica sands) in the different water velocity. To achieve this objective, we conducted a laboratory-scale column experiment to determine the amount of iron oxide nanoparticles in silica sands. For this, the test performed includes dynamic light scattering, zeta potential, Transmission Electron Microscopy (TEM) and ultraviolet-visible (UV-VIS). The classical Derjaguin-Landau-verwey-Overbeek (DLVO) and attachment efficiency is applied to assess and describe the interaction energy between particles and attachment between nanoparticles with collector surfaces.

II. MATERIALS AND METHOD

Fe_2O_3 was purchased from Sigma-Aldrich (Malaysia) in the form of powder with <50 nm diameter size (BET). Humic acid was also purchased from Sigma-Aldrich (Malaysia).

A. Humic acid - Fe_2O_3 Suspensions

A stock solution of humic acid with a concentration of 1 g/L was prepared by dissolving humic acid in deionised water for 24 h. The stock solution was then filtered through 0.45 μm filter paper using vacuum suction and stored at 4°C before experimental use. 100 mg/L concentration of humic acid was prepared by diluting the readymade stock solution with deionised water. The experiment was continued by adding 100 mg/L of Fe_2O_3 in 100 mg/L of humic acid. The solution was stirred for 24 h at room temperature. A fresh aliquot of samples with different pH (pH 3 – pH 9) was prepared. 0.1 M hydrochloric acid (HCL) or 0.1 M sodium hydroxide (NaOH) was added and adjusted until a required pH was obtained. To ensure the stability of the samples, the suspensions were left for 24 h and then centrifuged at 3000 rpm for 10 min before measurements were made.

B. Adsorption Experiments

The stability of nanoparticles in dispersion systems was evaluated through sedimentation experiments. The

sedimentation tests were conducted in static conditions. The kinetic aggregation process was monitored utilising a UV-VIS, measuring the sedimentation process nanoparticles via time-resolved optical absorbance. The absorbance of the samples was measured at a wavelength of 200 nm – 800 nm and was recorded for 180 min with different time intervals (i.e. 1 min, 5 min, 10 min, 20 min, 30 min, 45 min, 60 min, 75 min, 90 min, 120 min and 180 min). The experiments were carried out in duplicates and the results presented as the average of the data. The amount of natural organic matter adsorbed on the surface of nanoparticles was calculated using a linear equation (Chekli *et al.*, 2013a):

$$q(t) = (C_o - C_t)\frac{V}{m} \quad (1)$$

where C_o and C_t (mg/L) is the initial and concentration at time t of NOM in solution, V (L) is the solution volume, and m (g) is the mass of nanoparticles.

Adsorption data were fitted to the pseudo-first and pseudo-second-order kinetic models using linearised parameter estimations. The pseudo-second-order kinetic model showed functional correlations and was employed for data analysis.

$$\frac{t}{q(t)} = \frac{1}{kq_e^2} + \frac{1}{q_e} \quad (2)$$

where k (g/mg.min) is the rate of the pseudo-second-order and q_e (mg/g) is the amount of DOM adsorbed on the surface of nanoparticles at equilibrium. The k and q_e values obtained from the slope and intercept of the y-axis after plotting a straight line of t/q(t) against t respectively.

C. Porous Media Preparation and Column Transport Test

The porous media used for Fe_2O_3 nanoparticle transport experiment was silica sand (Kaolin (Malaysia) Sdn Bhd. The silica sand was sifted through 125 µm and 175 µm stainless steel sieves to achieve an average of the size of 150 µm. Silica sand was cleaned from impurities by soaking it in 1.0 M hydrochloric acid (HCL) for 24 hours, washing with deionised water and heating at 100 °C for 24 hours.

The cleaned silica sand (936.20 g) was packed into laboratory-scale column infiltration tests with an inner diameter of 5.2 cm and a length of 34 cm yielding a porosity of 53%. A 0.45 µm filter paper was placed at the inlet and outlet of the column to prevent migration during displacement tests (Esfandyari Bayat *et al.*, 2015). Three pore volumes (PVs) of deionised water were initially passed through porous media to ensure a homogenous saturation of pack at a constant velocity of 2.93 ml min^{-1} using a peristaltic pump (Watson Marlow 323 S). The suspensions (pH 7) were injected into the column at a constant velocity of 2.93 ml min^{-1} (natural water velocity in porous media) and effluent was collected continuously in 10 ml centrifuge tube. The experiments were repeated at a different velocity, which is 6.5 ml min^{-1} and 10 ml min^{-1} simulating rapid sand filtration (Chowdhury *et al.*, 2011) respectively. Effluent samples were analysed via Ultraviolet-Visible Spectroscopy (UV-VIS).

D. Characterisation of Nanoparticles Suspensions

1. Z-average hydrodynamic diameter and zeta potential measurements

The z-average hydrodynamic diameter and zeta potential of solutions were measured by Dynamic Light Scattering (DLS) technique with Zetasizer Nano (λ=633 nm, Malvern Instrument). To determine the z-average hydrodynamic diameter, an aliquot of 2 ml of suspensions solutions was injected into 12 mm o.d square polystyrene cuvettes (DTS 0012) and conducted for 5 min at 25 °C (room temperature). Three measurements for each suspension's solution were performed. Zeta potential measurements were conducted with folded capillary zeta cell (DTS 1070). Triplicate measurements were performed for each suspension solution at 5 min at room temperature, and an average of zeta potential was recorded.

2. Transmission Electron Microscopy (TEM) analysis

A fresh aliquot of 2 ml of suspensions (pH 3, pH 5, pH 7 and pH 9) that was used in z-average hydrodynamic diameter and zeta potentials were used for TEM analysis. Images of selected suspensions images were obtained from Philips CM12 Transmission Electron Microscope. One drop of the suspensions was placed on a copper grid, followed by ambient drying for 30 min before TEM analysis.

3. DLVO calculation

The Derjaguin-Landau-Verwey-Overbeek (DLVO) model is the most widely used model to describe the thermodynamic interaction between two particles in a suspension. This theory predicts the probability of two particles sticking together by the sum of van der Waals (V_{vdw}) force and electrostatic repulsive (V_{edl}) forces to get the total interaction energy (V_t). The sum of these two forces determines the net interaction between particles is repulsive or attractive. In short, if total interaction energy is negative, it represents the van der Waals that is more dominant than the electrostatic repulsive force. Hence, it will be more net attractive and vice versa.

$$V_t = V_{vdw} + V_{edl} \quad (3)$$

DLVO calculations formula is expressed as the following, according to Elimelech *et al.*, 1995. The van der Waals attractive energy and electrical double layer repulsive energy are expressed as follows.

$$V_{vdw} = -\frac{A_h r}{12s} \quad (4)$$

$$V_{edl} = 2\pi er\gamma^2 e^{-ks} \quad (5)$$

In which A_h is the Hamaker constant; 2.5 x 10^{-19} for Fe_2O_3 (De Mesquita *et al.*, 2003), r (m); is the radius of particles, s (m); separation distance between the surface of interacting particles, e; elementary charge of an electron, k; Debye length, γ; zeta potential.

4. Attachment efficiency

The attachment efficiency is defined as the ratio of the rate of particle deposition on a collector to the rate of collisions with that collector (Elimelech *et al.*, 1995). The attachment efficiency is presumed determined by the solution chemistry, existence of the nanoparticles and the collector surfaces; it is represented as:

$$\alpha = \frac{-4r_c}{3(1-\varepsilon)\eta_o} \ln \frac{c}{co} \quad (6)$$

where C and C_o are the concentrations of nanoparticles in the effluent and influent, respectively, passing through a column with a length of L, filled with media with a porosity of ε and collector radius of r_c (Lecoanet & Wiesner 2004). For single collector efficiency η_o, Tufenkji-Elimelech (TE) proposed a function comprised of three dimensionless numbers representative of removal by diffusion (η_P), interception (η_i) and gravitational sedimentation (η_G);

$$\eta_o = \eta_P + \eta_i + \eta_G \quad (7)$$

where

$$\eta_o = 2.4\, A_s^{1/3}\, N_R^{-0.081}\, N_{Pe}^{-0.715}\, N_{vdw}^{0.052} + 0.55\, A_s\, N_R^{1.675}\, N_A^{0.125} + 0.22\, N_R^{-0.24}\, N_G^{1.11}\, N_{vdw}^{0.053} \quad (8)$$

A_S is the Happel correction factor; N_{Pe} is the Peclet number; N_R is the interception number; N_{vdW} is the van der Waals number characterising ratio; N_A is the attraction number, and N_G is the gravitation number.

The maximum distance of those colloids may be transported in saturated porous media, L_{max},

$$L_{max} = \frac{-2d_c}{3(1-f)\alpha\eta_o} \ln [C/C_o] \quad (9)$$

III. RESULT AND DISCUSSION

A. Stability of Iron Oxide Nanoparticles Suspensions

Figure 1 shows the z-average hydrodynamic diameter of iron oxide nanoparticles suspension at a variety of pH values in the range between pH 3 and pH 9. As pH increases in the suspensions, the z-average hydrodynamic diameter decreases. Significant aggregation was found between pH 3 and pH 4 due to charge neutralisation between positive charges of iron oxide and negative charges of humic acid. Large aggregate settled down as sediment and can be observed with naked eyes within a few minutes while small aggregate (1604 – 2274 nm) was observed in Figure 1. Increasing pH in the suspensions made z-average hydrodynamic diameter to become smaller (88.81 – 98.5 nm) due to the stabilisation process (pH 5- pH 9). At low ionic strength and high pH, functional groups are fully ionised, and the nanoparticles charges linked by organic structure tend to move as far as possible from each other (Tombacz *et al.*, 2000)

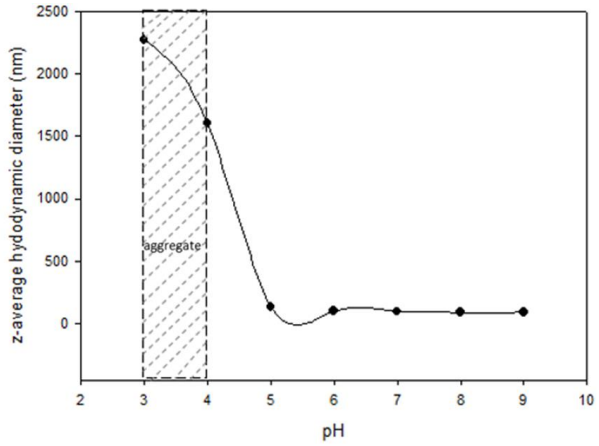

Figure 1. z-average hydrodynamic diameter of suspensions as a function of pH

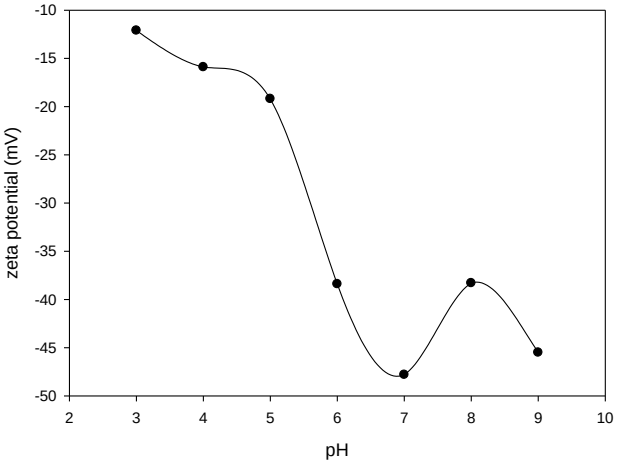

Figure 2. At pH 6 and above, iron oxide nanoparticles are highly negative charge and will be stable in the suspensions

Surface charge of suspensions are negative in the whole pH range studied, as shown in Figure 2. Zeta potentials measured at pH 3 until pH 5 were above -30 mV and below -30 mV for pH 6 and above. As a rule, zeta potentials value below – 30 mV provide enough force to keep nanoparticles in a suspension. Humic acid has a negative zeta potential at a whole pH (pH 3- ph 9). Iron oxide has a positive zeta potential below the point of zero charges, which is around pH 7 (Baalousha 2009; Labille & Brant 2010; Chekli *et al*., 2013a), and negative zeta potential above the point of zero charges. Point of zero charge is a pH at which particle surface is zero due to the absence of any positive or negatives charges. Humic acid covered the surface of iron oxide nanoparticles (Chekli *et al.* 2013b). It adsorbed onto the particles (Ramos-Tejada *et al*., 2003), thereby conferring negative surface charge across a wide range of pH values (Figure 2). The adsorption of humic acid will neutralise the positive charges and induce electrostatic destabilisation. Electrostatic destabilisation happens when particles initially have positives charges. In suspensions at pH 7, the adsorption humic acid imparts more negative surface charges onto iron oxides due to intrinsic negative charges of humic acid. While at pH above pH 7, electrostatic stabilisation occurs because iron oxide is negatively charged and as showed by a low of zeta potential value in Figure 2.

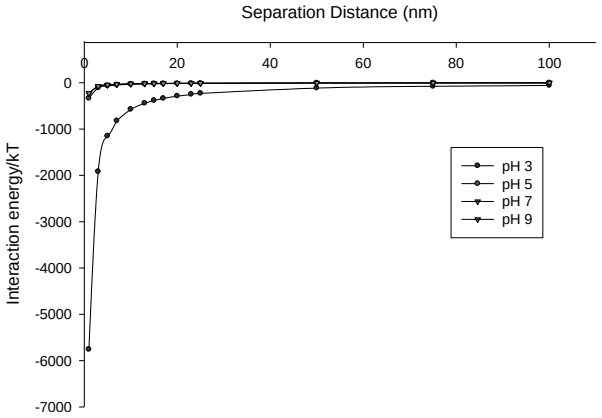

Figure 3. Interaction energy profiles for iron oxide nanoparticles as a function of pH according to DLVO theory

Plotted in Figure 3 are the DLVO interaction energy profiles for iron oxide NP-NP interaction as a function of pH. The DLVO theory explains the stability of nanoparticles dispersion in humic acid suspensions. High van der Waals attractions dominated at pH 3 resulting in the formation of large aggregate and have a low negative value of zeta potential. This can be explained according to DLVO theory as the significant decrease in surface charges, and NP aggregates in diffusion-limited mode, which, implies that each collision between primary and/or aggregate leads to particles sticking. Interaction energy decreases and approaches zero with increasing pH. Starting at pH 5 and above, the interaction energy between particles decreases.

Although the negative interaction energy which is van der Waals interaction energy exists, however, it is too low to enhance the aggregation of nanoparticles and enough energy

to prevent their aggregation. According to DLVO theory, the electrostatic barrier energy height between nanoparticle-nanoparticle is negative, indicating that there is an attraction force (VDW) between nanoparticle-nanoparticle. As a result of this attraction forces, the affinity of the nanoparticle to attach to the nanoparticle is high.

From z–average hydrodynamic diameter, zeta potential and interaction energy profile, the researchers conclude that nanoparticles will be aggregated and settle down as sediment at low pH levels (pH 3- pH 5). While at high pH, which is pH range of natural water (pH 6.5 – pH 8.5), nanoparticles are stable, mobile and transported.

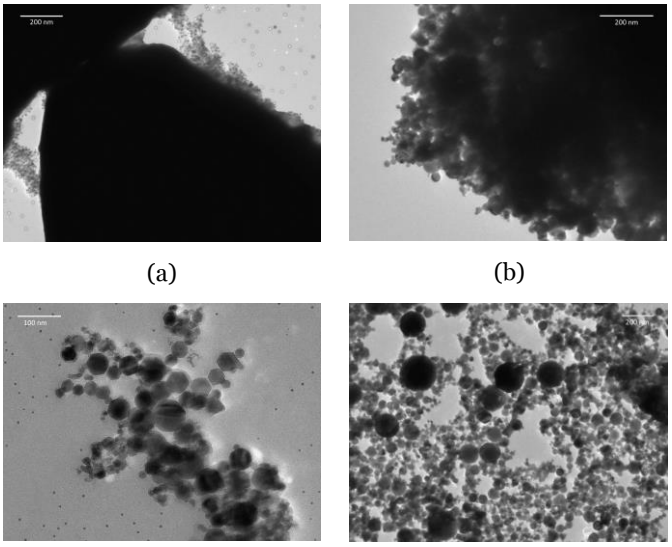

(a) (b)

(c) (d)

Figure 4. TEM images of suspensions (a) pH 3, (b) pH 5, (c) pH 7 and (d) pH 9

Figure 4(a) shows the large and small aggregates at pH 3, which is in good agreement with DLS result that shows two peaks, which was 2681 ± 2 nm for peak 1 and 73 ± 2 nm for peak 2. Dark areas represent dense aggregates while small aggregates occur as branches. Zeta potentials for pH 3 and pH 5 are -12.1 mV and -19.3 mV respectively indicating that suspension is unstable and will settle down as sediment due to large van der Waals attraction energy. The type of interaction play a role in the resulting aggregate structure, which has been described as spherical or chain (Kanel *et al*., 2007) like for the branch. The repulsive force required to stabilise particle dispersion against van der Waals force is derived from electrostatic double-layer repulsion and steric repulsion forces generated from the adsorption of long-chain polymers in the surface of particles (Godinez & Darnault 2011).

The formation of chain-like structures observed in Figure 4(c) is generally attributed to magnetic interactions between iron oxide nanoparticles. Halo effect appearances also observed in Figure 4(c) that increases electrostatic double-layer repulsive forces. Figure 4(d) shown the spherical structure and disaggregate at pH below PZC due to van der Waals force. Zeta potential for pH 7 (-46.7 mV) and pH 9 (-45.6 mV) have enough force to dispersed and maintain iron oxide nanoparticles in suspensions for long periods.

B. Transportation of Iron Oxide in Silica Sand

The adsorption kinetics of humic acid on iron oxide nanoparticles was fast for 180 min and the reaction a slower after that. This adsorption kinetics demonstrated that the adsorption of NOM on nanoparticle was faster under 180 min, where the aggressive reaction between negatively humic acid and positively iron oxide nanoparticles occurs. The amount of humic acid adsorbed on the surface of iron oxide nanoparticles at equilibrium was 75.93 mg/g.

The adsorption data were then fitted with the pseudo-second-order kinetic model, as shown in Figure 5(b). The results indicated that the correlation coefficient was higher than 0.95, and the calculated amount of NOM adsorbed on the surface of iron oxide nanoparticles at equilibrium. 75.75 mg/g was consistent with the experimental results (75.93 mg/g). This suggested that kinetic data are well described with a pseudo-second-order kinetic model, and the rate kinetic model was 0.2086 g/ (mg.min).

A breakthrough curves defined as the ratio of the actual concentration to the source of concentration. This curve reflects the fate of iron oxide nanoparticle-humic acid suspensions either deposited or discharged from the porous media column. Lower relative concentration (C/C_o) would result in more deposition of nanoparticles, resulting in higher α and η value. In contrast, higher relative concentration value will result in more nanoparticles discharged from the porous medium.

From Figure 6, the concentration of suspensions solution in the effluent increased with increasing flowrate velocity. Increase flowrate enhanced the mobility of nanoparticles and led to more elution due to aggregate breakup. Increased flow

rate velocity will increase the nanoparticles discharged from the porous medium and less deposited within the medium. Particle smaller than approximately 100 nm has very high efficiencies of transport to collector surface due to Brownian diffusion (Lecoanet & Wiesner 2004).

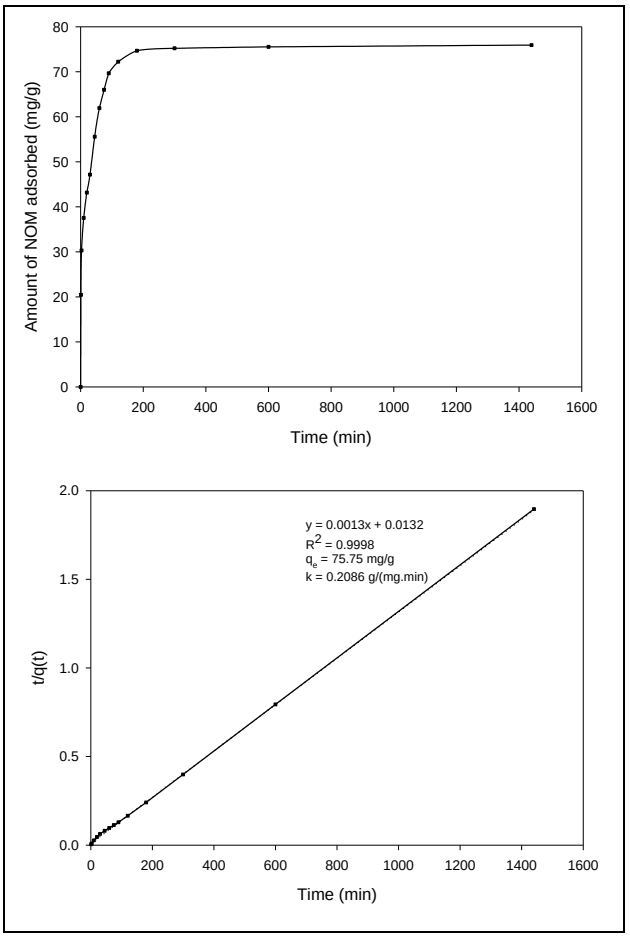

Figure 5. (a) Adsorption kinetics of humic acid on iron oxide nanoparticles at pH 7; (b) Pseudo second order kinetics models

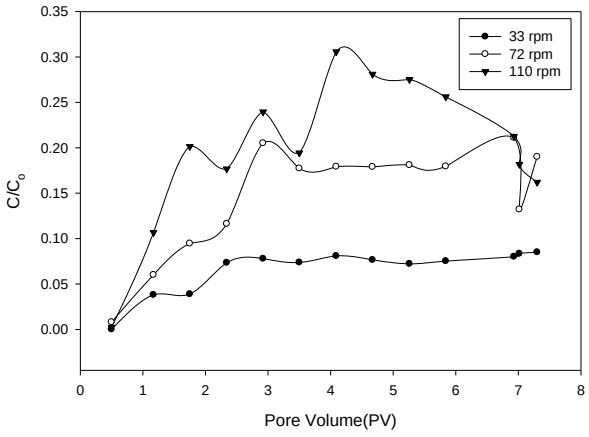

Figure 6. Breakthrough curves for iron oxide nanoparticles at three different velocities

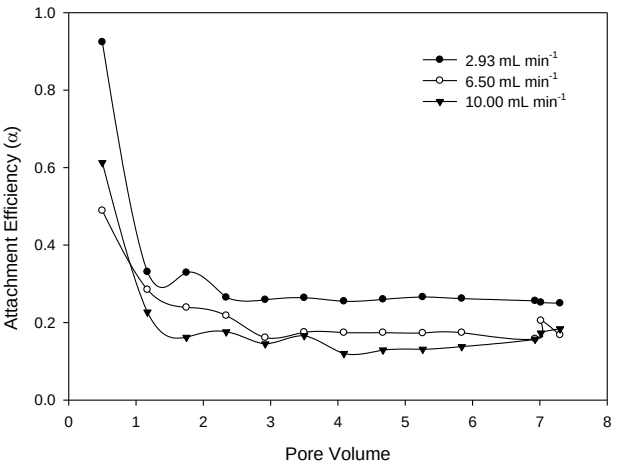

Figure 7. Attachment efficiency of iron oxide nanoparticles as a function of the pore volume

Figure 7 shows a profile of attachment efficiency of iron oxide nanoparticles as a function of pore volume at three different velocities. Increased velocity will induce a reduction in attachment efficiency and leads to more suspension of iron oxide in the effluent due to aggregate breakup. Particles are not strongly attached to the surface collector with increasing water velocity. Doubling the flow velocity increased the transport of iron oxide nanoparticles and decreased the attachment efficiency between nanoparticles and collector.

From this situation, can conclude that 2.93 ml min^{-1} flow velocity produced a high attachment efficiency compare to another velocity because of the presence of attachment energy generated by the sum of attractive between the particles and collector. Based on the calculation, the maximum distance that iron oxide nanoparticles may be transported in silica sand approximately 169-170 m.

IV. CONCLUSION

The aggregation and deposition behaviour of iron oxide nanoparticles in water and porous media were investigated through experimental techniques and modelling calculations (DLVO, pseudo-second-order kinetic model, attachment efficiency). In the presence of humic acid, in high pH (6-9) iron oxide nanoparticles achieve stability, mobile and will be transported. Meanwhile, it was observed that iron oxide nanoparticles settled down as sediment in low pH (3-4). The behaviour of these nanoparticles was consistent with the

prediction by DLVO model and image (TEM).

Based on research on the transport of iron oxide nanoparticles in silica sand, nanoparticles are discharged when the velocity increases. Nevertheless, in real environmental situation, groundwater moves very slowly in the subsurface (2.93 ml min^{-1}). From the attachment efficiency model, it is expected that most of the nanoparticles released into the subsurface will be aggregated and finally deposited in porous media. Meanwhile, in fast flow water velocity (6.50 ml min^{-1}, 10.00 ml min^{-1}), the attachment between collector and nanoparticle are weak and result in less deposited in porous media

V. ACKNOWLEDGEMENT

The authors would like to acknowledge the financial support received from Universiti Kebangsaan Malaysia under grant UKM-AP-2015-006 and centre for Research and Instrumentation (CRIM) for the support given.

VI. REFERENCES

Baalousha, M, 2009, 'Aggregation and disaggregation of iron oxide nanoparticles: influence of particle concentration, pH and natural organic matter', *The Science of the Total Environment*, vol. 407, no. 6, pp. 2093-2101.

Baalousha, M, Manciulea, A, Cumberland, S, Kendall, K, Lead, JR, 2008, 'Aggregation and surface properties of iron oxide nanoparticles: influence of pH and natural organic matter', *Environmental toxicology and chemistry*, vol. 27, no. 9, pp. 1875-1882.

Buffle, J, Wilkinson, KJ & Stoll, S, 1998, A Generalised Description of Aquatic Colloidal Interactions: The Three-colloidal Component Approach, *Environ. Sci. Technol.*, vol. 32, no. 19, pp. 2887-2899.

Bundschuh, M., Filser, J., Lüderwald, S., McKee, M. S., Metreveli, G., Schaumann, G. E., Schulz, R., *et al.* 2018. 'Nanoparticles in the environment: where do we come from, where do we go to?', *Environmental Sciences Europe*, vol. 30, no. 6, pp. 1-17.

Chekli, L, Phuntsho, S, Roy, M, Shon, HK, 2013a, 'Characterisation of Fe-oxide nanoparticles coated with humic acid and Suwannee River natural organic matter', *The Science of the Total Environment*, vol. 461-462, pp. 19-27.

Chekli, L, Phuntsho, S, Roy, M, Lombi, E, Donner, E, Shon, HK, 2013b, 'Assessing the aggregation behavior of iron oxide nanoparticles under relevant environmental conditions using a multi-method approach', *Water Research*, vol. 43, no. 13, pp. 4585-4899.

Chowdhury, L, Hong, Y, Honda, RJ, Walker, SL, 2011, 'Mechanism of TiO2 nanoparticles transport in porous media: Role of solution chemistry, nanoparticle concentration, and flowrate', *Journal of Colloid and Interface Science*, vol. 360, no. 2, pp. 548-555.

De Mesquita, LMS, Lins, FF, Torem, ML, 2003, 'Interaction of hydrophobic bacterium strain in an hematite next term quartz flotation system', *International Journal of Mineral Processing,* vol. 71, no. 1-4, pp. 31-44.

Dickson, D, Liu, G, Li, C, Tachiev, G, Cai, Y, 2012, 'Dispersion and stability of bare hematite nanoparticles: effect of dispersion tools, nanoparticles concentration, humic acid and ionic strength', *The Science of the Total Environment*, vol. 419, pp. 170-177.

Elimelech, M, Gregory, J, Jia, X, Williams, RA, 1995, *Particle deposition and aggregation: measurement, modelling & Simulation*, Butterworth-Heinemann, USA.

Esfandyari, BA, Junin, R, Shamshirband, S, Tong, CW, 2015, 'Transport and retention of engineered Al_2O_3, TiO_2, SiO_2, nanoparticles through various sedimentary rocks', *Scientific Report*, vol. 5, pp. 1-12.

Frimmel, FH, Niessner, R (eds) 2010, *Nanoparticles in the water cycle: Properties, analysis and environmental relevance*, Springer Heidelberg Dordrecht London, New York US.

Ghosh, S, Mashayekhi, H, Bhowmik, P, Xing, B, 2010, 'Colloidal stability of Al2O3 nanoparticles as affected by coating of structurally different humic acids', *Langmuir*, vol. 25, no. 2, pp. 873-879.

Godinez, IG, Darnault, CJG, 2011, 'Aggregation and transport of nano-TiO in saturated porous media: Effects of pH, surfactants and flow velocity', *Water Research*, vol. 45, no. 2, pp. 839-851.

Hoecke, KV, Schamphelaere, KACD, Mereren, PVD, 2011, 'Aggregation and ecotoxicity of CeO2 nanoparticles in synthetic and natural waters with variable pH, organic

matter concentration and ionic strength', *Environmental Pollution*, vol. 30, no. 4, pp. 1-27.

Hotze, EM, Phenrat, T, Lowry, GV, Mellon, C, 2010. 'Nanoparticle aggregation: challenges to understanding transport and reactivity in the environment', *J. Environ. Qual*, vol. 29, pp. 1909-1924.

Hu, JD, Zevi, Y, Kou, XM, Xiao, J, Wang, XJ, Jin, 2010, 'Effect of dissolved organic matter on the stability of magnetite nanoparticles under different pH and ionic strength conditions', *The Science of the total environment,* vol. 408, no. 16, pp. 3477-3489.

Jeong, SW, Kim, SD, 2009, 'Aggregation and transport of copper oxide nanoparticles in porous media', *Journal of Environmental Monitoring: JEM*, vol. 11, no. 9, pp. 1595-1600.

Ju-Nam, Y, & Lead, JR, 2008. 'Manufactured nanoparticles: An overview of their chemistry, interactions and potential environmental implications', *Science of the Total Environment*, vol. 400, no. 1-3, pp. 396-414.

Kanel, SR, Nepal, D, Manning, B, Choi, H, 2007. 'Transport of surface-modified iron nanoparticle in porous media and application to arsenic (III) remediation', *Journal of Nanoparticle Research*, vol. 9, no. 5, pp. 725-735.

Klaine, SJ, Alvarez, PJJ, Batley, GE, Fernandes, TF, Handy, RD, Lyon, DY, Mahendra, S, 2008. 'Nanomaterials in the environment: behavior, fate, bioavailability, and effects', *Environmental Toxicology and Chemistry,* vol. 27, no. 9, pp. 1825-1851.

Labille, J. & Brant, J, 2010, 'Stability of nanoparticles in water', *Nanomedicine*, vol. 5, no. 6, pp. 985-998.

Lecoanet, HF & Wiesner, MR, 2004, 'Velocity effects on fullerene and oxide nanoparticle deposition in porous media velocity effects on fullerene and oxide nanoparticle deposition in porous media', *Environmental Science & Technology*. vol. 38, no. 713, pp. 4377-4382.

Nur, SA, Shahidan, R, Wan, ZWY, 2019, 'Aggregation and stability of iron oxide and alumina nanoparticles: Influence of pH and humic acid concentration', *Sains Malaysiana*, vol. 48, no. 2, pp. 435-442.

Omar, FM, Aziz, HA, Stoll, S, 2014, 'nanoparticle properties, behavior, fate in aquatic systems and characterisation methods nanoparticle properties, behavior, fate in aquatic systems and characterisation methods', *Journal of Colloid Science and Biotechnology,* vol 3, pp. 1-30.

Peijnenburg, WJGM, Baalousha, M, Chen, J, Chaudry, Q, Von Der Kammer, F, Kuhlbusch, TaJ, Lead, J, 2015, 'A review of the properties and processes determining the fate of engineered nanomaterials in the aquatic environment', *Critical Reviews in Environmental Science and Technology,* vol. 3389, pp. 2084-2134.

Petosa, AR, Brennan, SJ, Rajput, F, Tufenkji, N, 2012, 'Transport of two metal oxide nanoparticles in saturated granular porous media: Role of water chemistry and particle coating', *Water Research*, vol. 46, no. 4, pp. 1273-1285.

Ramos-Tejada, MM, Ontiveros, A, Viota, JL, Durán, JDG, 2003, 'Interfacial and rheological properties of humic acid/hematite suspensions', *Journal of Colloid and Interface Science,* vol. 268, no. 1, pp. 85-95.

Tombacz, E, Dobos, A, Szekeres, M, Narres, HD, Klumpp, E, Dekany, I, 2000, 'Effect of pH and ionic strength on the interaction of humic acid with aluminium oxide', *Colloid Polym. Sci.*, vol. 278, pp. 337–345.

Wagner, S, Gondikas, A, Neubauer, E, Hofmann, T, Von Der Kammer, F, 2014, 'Spot the difference: Engineered and natural nanoparticles in the environment-release, behavior, and fate', *Angewandte Chemie - International Edition*, vol. 53, no. 46, pp. 12398–12419.

Yang, K, & Xing, B, 2009, 'Interactions of humic acid with nanosized inorganic oxides', *Environmental Pollution*, vol. 157, no. 4, pp. 1095—1100.